Volume 10 | Number 25 | 7 July 2019 | Pages 6223–6394

Chemical Science

rsc.li/chemical-science

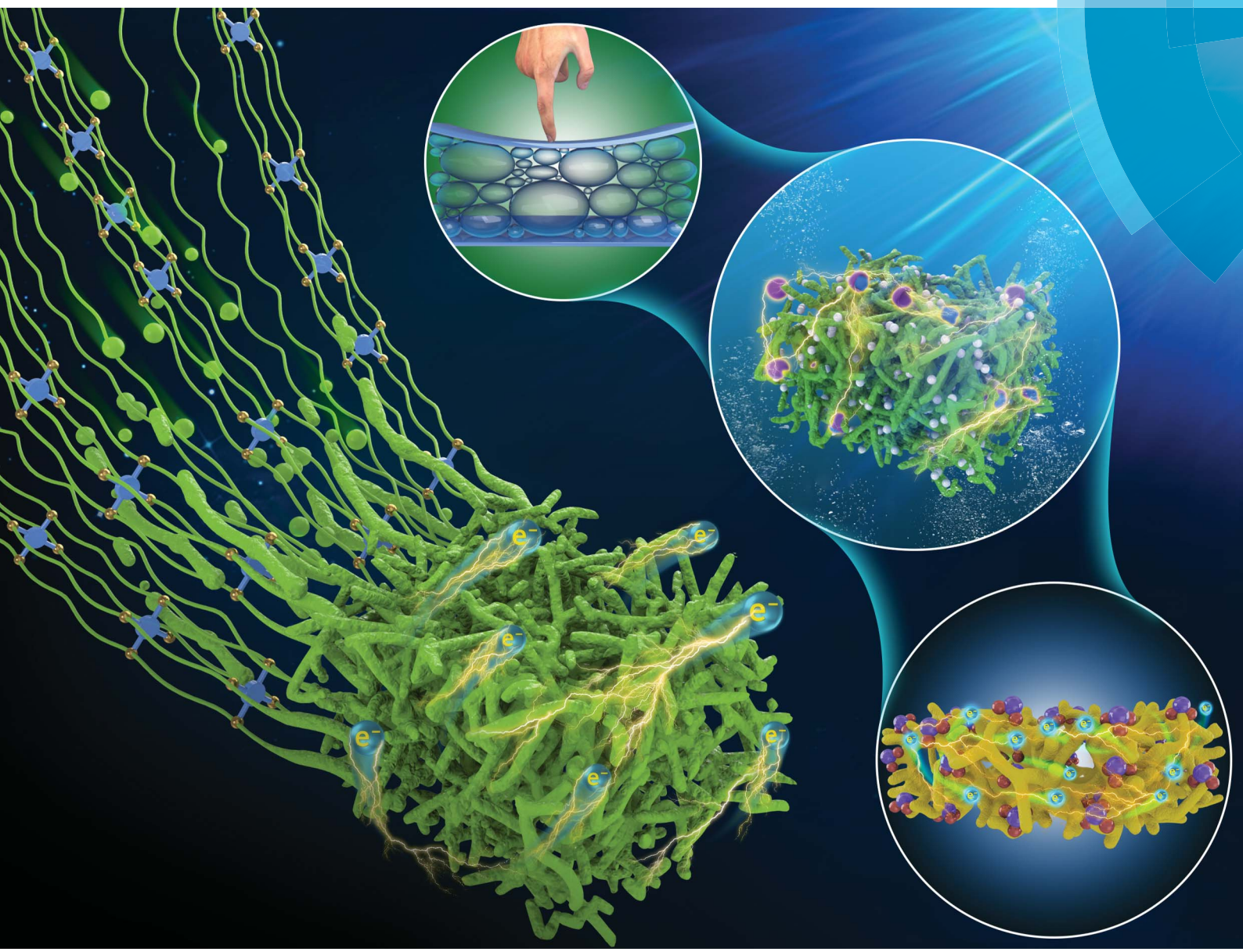

ISSN 2041-6539

ROYAL SOCIETY OF CHEMISTRY | Celebrating IYPT 2019

PERSPECTIVE
Lijia Pan, Guihua Yu *et al.*
Doping engineering of conductive polymer hydrogels and their application in advanced sensor technologies

Chemical Science

PERSPECTIVE

View Article Online
View Journal | View Issue

Cite this: *Chem. Sci.*, 2019, **10**, 6232

All publication charges for this article have been paid for by the Royal Society of Chemistry

Doping engineering of conductive polymer hydrogels and their application in advanced sensor technologies

Zhong Ma,†[a] Wen Shi,†[b] Ke Yan,[ab] Lijia Pan *[a] and Guihua Yu *[b]

Conductive polymer hydrogels are emerging as an advanced electronic platform for sensors by synergizing the advantageous features of soft materials and organic conductors. Doping provides a simple yet effective methodology for the synthesis and modulation of conductive polymer hydrogels. By utilizing different dopants and levels of doping, conductive polymer hydrogels show a highly flexible tunability for controllable electronic properties, microstructures, and structure-derived mechanical properties. By rationally tailoring these properties, conductive polymer hydrogels are engineered to allow sensitive responses to external stimuli and exhibit the potential for application in various sensor technologies. The doping methods for the controllable structures and tunable properties of conductive polymer hydrogels are beneficial to improving a variety of sensing performances including sensitivity, stability, selectivity, and new functions. With this perspective, we review recent progress in the synthesis and performance of conductive polymer hydrogels with an emphasis on the utilization of doping principles. Several prototype sensor designs based on conductive polymer hydrogels are presented. Furthermore, the main challenges and future research are also discussed.

Received 24th April 2019
Accepted 28th May 2019

DOI: 10.1039/c9sc02033k

rsc.li/chemical-science

1. Introduction

Conductive polymer hydrogels (CPHs) have emerged as a promising platform for bioelectronic and electronic interfaces, with intrinsic biocompatibility, high electronic/ionic conductivity, and excellent mechanical properties.[1–3] There have been remarkable advances in developing CPHs, such as those containing polyaniline (PAni), polypyrrole (PPy), poly(3,4-ethylenedioxythiophene) (PEDOT), and polythiophene (PTh).[4,5] These hydrogels have exhibited tunable microstructures and chemical/physical properties, which enable broad applications in sensors,[6,7] energy storage,[8–11] solar vapor generation,[12,13] dynamic drug delivery,[14–16] and repellent surfaces.[17,18]

Compared with conventional solid-state polymers, CPHs synergize the advantageous features of both hydrogels and organic conductors.[19–21] It is worth noting that hydrogels and

[a]*Collaborative Innovation Center of Advanced Microstructures, Jiangsu Provincial Key Laboratory of Photonic and Electronic Materials, School of Electronic Science and Engineering, Nanjing University, 210093 Nanjing, China. E-mail: ljpan@nju.edu.cn*

[b]*Materials Science and Engineering Program, Department of Mechanical Engineering, The University of Texas at Austin, Austin, Texas 78712, USA. E-mail: ghyu@austin.utexas.edu*

† These authors contributed equally to this work.

Zhong Ma received his B.S. in microelectronics from Nanjing University in 2016. He is currently a Ph.D. candidate in Electronic Science and Technology working under the direction of Professor Lijia Pan. His research interests include polymer sensors and flexible electronics.

Wen Shi is a Ph.D. student in Prof. Guihua Yu's group at The University of Texas at Austin. She received her B.S. in Materials Physics from the University of Science and Technology of China. Her current work in Prof. Yu's lab focuses on the synthesis and modification of conductive polymer hydrogels designed for energy conversion and storage.

conductive polymers are two typical kinds of smart materials, also named as intelligent or responsive materials, which are designed materials with chemical or physical properties that can be significantly changed in response to external stimuli (such as temperature, pH, stress, moisture, electric fields, magnetic fields, light, chemical compounds, *etc.*). Unlike traditional dry-engineering materials and liquid-phase electrolytes, nanostructured conductive polymers, along with the high water content of hydrogels, offer a unique combination of properties that are not available in any other material.[22,23] The combined properties of both materials provide the potential for advanced sensor technologies.

Moreover, the morphology and physical/chemical properties of CPHs are easily modulated and controlled by the utilization of doping principles during the synthesis process. Doping, which allows for tuning the electronic properties of semiconductors, is a central method in the modern semiconductor industry. However, the doping of conductive polymers is substantially different from that of their inorganic analogs:[24,25] (1) the doping of conjugated polymers is mainly accomplished by charge-transfer redox chemistry or acid–base chemistry (protonation). For example, protonation through acid–base chemistry is often utilized in reversible chemical doping of PAni. The acidic dopant protonates the imine groups in PAni and leads to a polaronic (with spin) or bipolaronic (without spin) structure along the polymer chain, or an equilibrium between polarons and bipolarons;[26–28] (2) the doping levels in conductive polymers are significantly higher than the trace doping levels in inorganic semiconductors. The PAni doped with proton acid exhibits a conversion from an emeraldine base (EB) to an emeraldine salt (ES) form and an increase in conductivity of approximately 10^{10}.[25] In addition, such a large doping level makes it possible to introduce new functions into the polymer. Cao *et al.* synthesized conductive polymers with solution processability by using long-chain fatty acids to dope PAni;[29] (3) conductive polymers exhibit reversible doping/dedoping properties under the immediate stimuli of environments, allowing for dynamic electrical properties over a wide range from insulating to semiconducting and metallic changing. These properties establish doping as an important tool for developing advanced polymeric sensors; (4) doping introduces crosslinking, steric effects, and self-assembly effects, which enable a high tunability of polymer microstructures to enhance and/or add functions to CPHs. For example, using dopant molecules with different structures can be favorable for producing PPy with morphologies of nanoparticles, nanofibers, and foam-like nanostructures, which is attributed to the steric effects and electrostatic interaction.[30]

The controllable properties available with doping engineering make CPHs smart materials that are sensitive to various stimuli, change in response to the environment and are expected to have great potential for sensor applications, such as biosensors,[31,32] gas sensors,[7] and flexible force/strain sensors.[33] CPH-based sensors have been proven to have excellent sensing performances such as good sensitivity, quick response, low

Ke Yan received his B.Sc. degree in Applied Physics from Northeastern University, China. He joined Prof. Lijia Pan's group at Nanjing University to pursue his Ph.D. in Electronic Science and Engineering. He currently works under the supervision of Prof. Guihua Yu at The University of Texas at Austin as a visiting scholar. His current research interests focus on novel materials and devices for energy storage, flexible pressure sensors and oil/water separation for environmental remediation.

Lijia Pan is a Professor at the School of Electronic Science and Engineering, Nanjing University, China. He received his B.S. degree in Polymer Science and Engineering from South China University of Technology, and obtained his Ph.D. in polymer physics from the University of Science and Technology of China in 2003. He was a visiting professor in Prof. Zhenan Bao's group at Stanford University in 2011–2012 and 2017. He received the National Natural Science Fund for distinguished young scholars (2019–2023). His research interests include: conducting polymers and E-skin devices.

Guihua Yu is a Professor of Materials Science and Engineering and Mechanical Engineering at the University of Texas at Austin. He is a Fellow of the Royal Society of Chemistry, Sloan Research Fellow, and Camille Dreyfus Teacher-Scholar. He received his B.S. degree with the highest honor from the University of Science and Technology of China (USTC) and Ph.D. from Harvard University, followed by postdoctoral research at Stanford University. His research has been focused on the rational design, synthesis, and self-assembly of functional nanostructured organic and hybrid organic–inorganic materials for advanced energy and environmental technologies.

detection limit, and stability, demonstrating the potential of CPHs in advanced sensor technologies.[34]

In this perspective, we review and highlight the effects of doping strategies targeting the precise manipulation of CPHs' properties. We critically present typical and novel sensor designs based on CPHs, showing their outstanding advantages and great potential for applications in the sensor field.

2. Mechanism of doping-enabled modulation

Chemical or electrochemical polymerization has often been applied to build micro/nanostructured polymer hydrogels.[35] Compared with traditional template-directed polymer synthesis methods, doping modulation can be a straightforward and efficient method for CPH syntheses and property regulation through introducing charge and polymer interactions without the use of electrically insulating compounds.[36,37]

Generally, charge injection can be accomplished to make the polymer positively (p-doping) or negatively (n-doping) charged in a variety of ways, including chemical, electrochemical, photo, and metal–polymer interfacial doping. In the doping process, redox charges are supplied to the conducting polymer from the dopants, electrodes, photo-absorption, and other charge injections, and ions diffuse out of/into the polymer structure to compensate the electronic charges. In addition, the counter ions with functional groups are "surfactants" and play an important role in the interaction of polymers (*e.g.*, crosslinking, steric effects, and electrostatic interaction) and network morphology assembly.[38] Multivalent metallic ions can be used to crosslink the long-chain dopants of conductive polymers for the self-assembly synthesis method of CPHs, as was proposed by Inganäs *et al.*[39–41] The doping engineering enables CPHs to possess unique and novel properties that are not available from other materials and show a fundamental application in the sensor field (Fig. 1). Herein, we review the effect of doping on modulating the structures and properties of CPHs.

2.1 Doping-induced molecular self-assembly

Micro/nanostructuring has received intensive attention in the past few decades. However, most nanomaterials were synthesized in powder form and had to be refabricated into thin films with the help of adhesives or other compounds because most of the materials in the devices were used as thin films. Additionally, the additives reduced the physical properties and effective surface-to-volume ratio. Doping engineering provides molecular scale design of CPHs as an alternative low-temperature and solution-processed self-assembly method to form nanostructured thin films in either a wet or dry form.

The functional groups in the dopant molecules act as a crosslinker and gelator and contribute to a controllable self-assembled network morphology in the hydrogels. As previously reported, dopants of small molecules (*e.g.*, HCl, and H_2SO_4) can result in a morphology of nanoparticles of PAni, while large molecules tend to form nanofibers.[42,43] We reported a hierarchical nanostructured conducting PAni hydrogel with phytic acid as the dopant.[44] Each phytic acid molecule can interact with more than one PAni chain, which contributes to interconnecting nanostructures. Three-dimensional (3D) porous foam-like nanostructures are constructed from uniform coral-like nanofibers with a diameter of 60–100 nm (Fig. 2a). This facile synthesis route is easy to implement simply by mixing an oxidative initiator with an aniline monomer and phytic acid.[17]

This doping-induced self-assembly strategy can be extended to prepare various morphology-controlled CPHs with different types of dopants. Wang *et al.* reported a dopant-enabled approach for PPy hydrogels using copper phthalocyanine-3,4′,4″,4‴-tetrasulfonic acid tetrasodium salt (CuPcTs).[30] Based on electrostatic interactions and supramolecular self-assembly, PPy tends to grow into one-dimensional (1D) nanofibers with a self-sorting mechanism. The disc-like shape and sulfonic-acid functional groups of the dopant played an indispensable role in assembling the molecularly microstructured framework (Fig. 2b). By applying different types of dopants, the PPy hydrogels exhibited various morphologies of 1D nanofibers, nanoparticle necklaces, and granular particles. In addition, the polymerization time and concentration of CuPcTs have an effect on controlling the diameter of the nanofibers.

Based on controllable morphology, nanostructured CPHs tend to exhibit additional advantageous structure-derived properties, such as improved mechanical properties, a high surface-to-volume ratio, and a high electrical/ionic conductivity arising from shortened pathways for charge/ion transport.[45,46] Therefore, the nanostructure self-assembly of CPHs based on doping engineering serves as an effective method to obtain the properties required for improving the performances of CPH-based sensors.

2.2 Modulation of conductivity

A high conductivity is beneficial to achieving excellent sensitivity and stability in CPH-based sensors. Doping is the main process to improve the CPHs' electrical properties to those of a metal.[30,44] Doping introduces charge carriers of a relatively higher density into the polymer structures, which are able to move along the interconnected 3D network.[47]

The choice of dopant, doping strength, and doping level determine the conductivity of CPHs. For PAni, the doping level is related to the extent of polymer protonation, which determines the conductivity. The reversible acid–base doping/dedoping process enables efficient control over the insulator–metal transition between the EB and ES forms of PAni.[48] This simple and reversible transition in conductivity is favorable for introducing novel sensing functions and has applications in chemical sensors.[7]

The doping-induced nanostructures are able to enhance the interchain charge transport. Our phytic-acid-doped PAni hydrogel showed an electronic conductivity with a high value (0.11 S cm^{-1} for the wet hydrogel and 0.23 S cm^{-1} for the dried powder). Similarly, the CuPcTs-doped PPy showed a two-order increase in conductivity (7.8 S cm^{-1}) compared with that of pristine PPy and is tunable over a wide region. The electrostatic

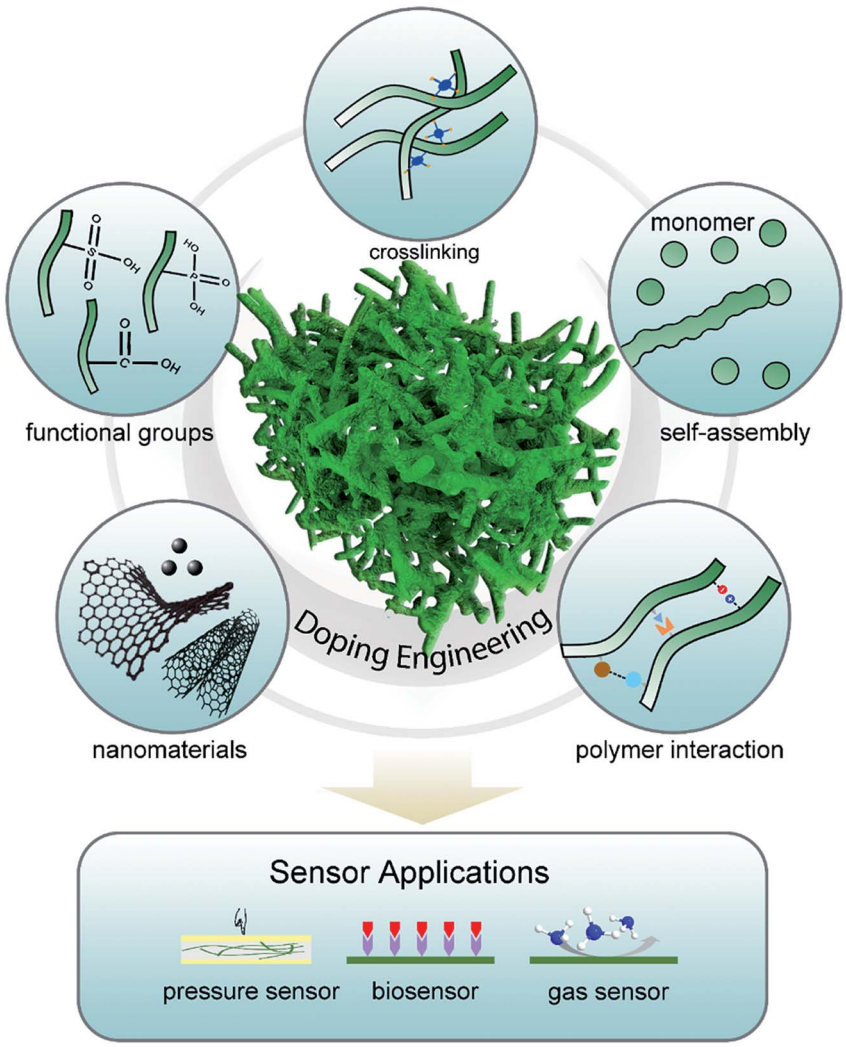

Fig. 1 Schematic illustration of the mechanism of doping engineering, modulation of properties of CPHs and advanced sensor applications. Dopant molecules with functional groups and counter ions can introduce some interactions (crosslinking, steric effects, and electrostatic interaction) among polymer structures. CPH-based hybrid materials incorporated with other nanomaterials further enhance the properties and their potential for sensor applications.

interactions between the tetra-functional CuPcTs and the PPy chains allow for a self-assembly mechanism that aligns the PPy chains to form 1D nanostructured PPy, whereas the long-range organization of parallel polymer chains is favorable for the electrical conductivity.[30] Furthermore, the dopant CuPcTs is an organic conductor and also improved the interchain charge transport of PPy. The conductivity of CPHs can be tuned over a wide range (~15 orders) by controlling its doping level.[49]

Moreover, hybrid inorganic–organic gel frameworks with a networked structure are capable of further improving the conductivity of CPH-based composite materials. For example, we recently reported a conductive gel framework material composed of CuPcTs-doped PPy and commercial lithium iron phosphate particles.[50] The hybrid gel achieved both high electronic and ionic conductivities (the Warburg coefficients for the hybrid gel framework is 91 $\Omega\ s^{-1/2}$). In addition to the high doping level and conjugated polymer chains, the continuous interconnected network also plays an important role in facilitating the electron transport.

2.3 Modulation of mechanical properties

Dense polymers suffer from mechanical brittleness due to their rigid conjugated-ring backbones, which hinder their application in flexible devices when no flexible side chains were introduced into the polymer.[51] CPHs with doping engineering provide a novel method to modulate the mechanical properties of conductive polymers by forming a hydrogel and by microstructure engineering, which enables novel prototype flexible electronic devices.

Mechanical flexibility was obtained with hollow nanospheres of CPHs because the porous microstructure possesses a structure-derived elasticity that is capable of accommodating the deformation and strain.[52] A hollow-sphere structure enables CPHs to exhibit a tunable effective elastic modulus.[33]

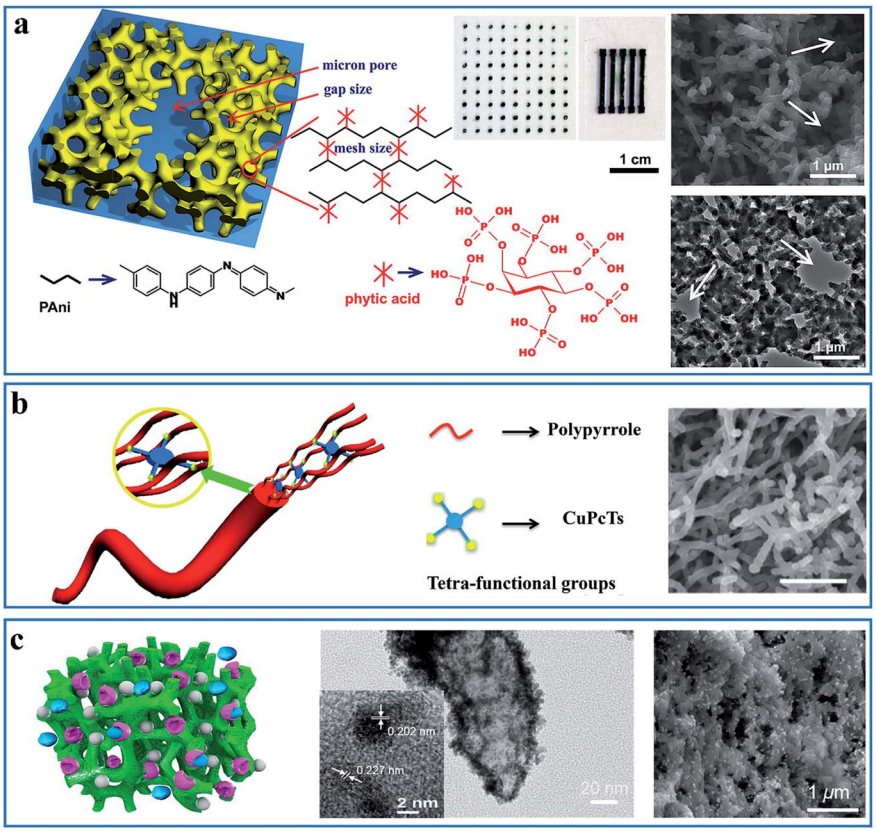

Fig. 2 Demonstration of the interaction and self-assembly effect between dopant molecules and polymer chains. (a) Schematic illustration (left) and scanning electron microscopy (SEM) and transmission electron microscopy (TEM) images (right) of the PAni hydrogel gelated and doped with phytic acid. The middle is the mask-spray-coated electrode array of the PAni hydrogel. Reprinted with permission from ref. 44 (copyright 2012 National Academy of Sciences). (b) A schematic illustration of the controlled synthesis of the CuPcTs-doped PPy hydrogel (left) and its SEM image (right, scale bar: 1 μm). Reprinted with permission from ref. 30 (copyright 2015 American Chemical Society). (c) A schematic illustration of the nanostructured PAni hydrogel incorporated with enzymes and Pt nanoparticles (left) and its TEM (middle) and SEM (right) images. Reprinted with permission from ref. 32 (copyright 2015 American Chemical Society).

With phytic acid as the dopant, a multiphase reaction mechanism was utilized to prepare hollow-sphere PPy (Fig. 3a). The effective elastic modulus of the microstructured PPy was measured to be 0.19 MPa (at 5 kPa), which is lower than the value of various polymer-based foams and capable of withstanding large strains and stresses (Fig. 3b). According to a recent study of Lu *et al.*, PPy hydrogels show an extraordinary elasticity with a compressive strain larger than 70%, which stems from the gradual maturation of the PPy network.[53] During the second growth process, micro-protrusions appear on the surface of the initial nanoparticles inhomogeneously, and they further grow into branches, finally resulting in randomly jointed ginger-like building blocks, which have been proven to contribute to structural superelasticity.[54,55] Additionally, the unique microsphere phases serve as microscale joint regions that dramatically reinforce the strength and enhance the energy dissipation, leading to a high stretchability (strain exceeding 600%) as well as an excellent mechanical strength and stability.[56]

In addition, the co-crosslinking of a dually synergistic network has provided an effective way to improve the flexibility of CPHs. Based on the flexible co-crosslinked structure of two kinds of intertwined gels, the mechanical strength can be controlled by adjusting the ratio of the different CPHs.[57,58] Incorporating nanosized active materials such as graphene and carbon nanotubes to form strong macromolecular interactions is another versatile approach to achieve uniform interconnectivity, flexibility, and stretchability.[10,59,60] The hybrid materials show great interconnectivity and an enhanced flexibility resulting from the strong macromolecular interactions between the CPHs and nanomaterials (Fig. 3c and d).

2.4 Stability enhancement

Owing to gelated nanostructures and the mechanism of contact resistance, the electrical connections within the 3D porous structures remained stable, even with the temperature-induced thermal expansion of the material.[61] In addition, nonvolatile dopants are difficult to remove, especially in the high-temperature range, and the crosslinking effect is able to weaken the impact of the environment, promoting the long-term stability of CPHs.[33,62] The piezoresistance of our phytic-acid-doped PPy showed negligible temperature-dependence and a signal drift in the range of −10 °C to 100 °C, revealing

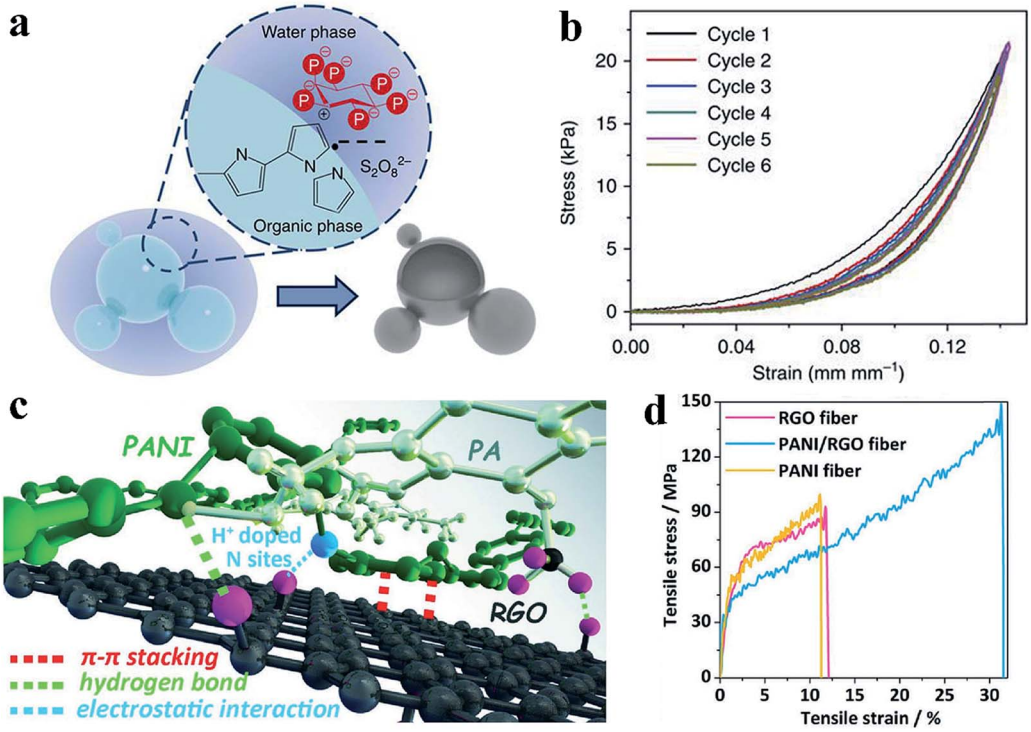

Fig. 3 Demonstration of the improved mechanical properties of the CPH-based materials. (a) Schematic of the interphase synthesis mechanism of PPy hydrogels. The hollow-sphere PPy is synthesized through a multiphase reaction between an aqueous solution of an oxidative reagent and pyrrole monomer solution, with phytic acid molecules acting as dopant and crosslinker. (b) Consecutive compression tests show the elasticity of the PPy film, which is due to the interconnected hollow-sphere nanostructures. Reprinted with permission from ref. 33 (copyright 2014 Macmillan Publishers Limited). (c) Demonstration of the possible interactions (electrostatic interaction, hydrogen bond, and π−π stacking) among a hybrid material of PAni, phytic acid, and reduced graphene oxide. (d) The strain–stress curves show the improved mechanical strength of the hybrid material. Reprinted with permission from ref. 10 (copyright 2018 Wiley).

its potential for use in harsh-temperature ambient environments. In addition to temperature stability, the high-weight phytic acid dopant also resulted in stability over time, with a resistance change of 77% after storage for 10 months.

Based on dopant-enabled 3D nanostructures, the immobilization and incorporation of a second component (*e.g.*, appropriate biomolecules and metal nanoparticles) can enhance the functionality of CPHs.[31,63] For example, porous nanostructures can improve the enzyme loading efficiency and immobilization strength in biosensors under mechanical deformation (Fig. 2c).[32,64] The improved adsorption and stability can reduce the amount of wasted enzyme. The incorporation of silicon or metal nanoparticles into CPHs can help build a continuous electron transport network for high conductivity, and the hierarchical nanostructures can accommodate the volume expansion of the nanoparticles.[32] The 3D wrapping of the particles has also been proven to achieve more-stable cycling performances.[61,63]

3. CPHs for advanced sensors

CPHs have been utilized in a variety of advanced sensors responding to different types of stimuli, such as pressure, metabolites, and gases. The key function of CPH-based sensors is to respond to external stimuli with a corresponding change in the electrical signal output. Here, we review the recent advances in CPH-based sensor applications including pressure sensors, biosensors, and gas sensors and discuss how the devices adopt the advantages of the doping method.

3.1 Flexible force/strain sensor

The flexible force/strain sensor is an electronic device inspired by human skin; the device includes pressure, tension, and strain sensors and releases an electrical signal output in response to mechanical deformation and applied forces, similar to what human skin does.[65,66] The key parameters to evaluate force sensors include sensitivity, response speed, and stability with cycling under force loading. Highly sensitive force/strain sensors can be applied in human health monitoring, prosthetic electronic skin, and human/machine interfaces.[67] In addition, a fast response and reduced hysteresis are beneficial for accurate and high-precision dynamic sensing.[68,69] Flexible piezoresistive sensors combining a conductor and soft materials have been developed due to advantages such as excellent stretchability, high sensitivity, fast responses, and excellent stability, as well as facile preparation, integration, and signal detection.[70,71]

Suitable mechanical properties are always critical when designing pressure sensors with an excellent performance.

CPHs, possessing hydrophilicity, high conductivity, mechanical flexibility, and stability, are competent candidates for wearable pressure sensors.[33] It has been demonstrated that porous structures are beneficial to increasing the sensitivity and deformability of thin-film-based mechanical sensors.[72] For example, we designed an elastic microstructured conductive PPy for use in a remarkable pressure sensor, which utilized the contact resistance sensing mechanism at the interface between the polymer and electrode (Fig. 4a).[33] The hollow-sphere-structured PPy, with phytic acid as the dopant, was obtained through a multiphase synthesis technique of mixing reagents in different phases. The spherical shell geometry enabled the inherently brittle PPy to be elastically deformed with a low effective modulus. The patterned PPy-based pressure sensor could detect pressures as low as 0.8 Pa and presented advantages including an ultrahigh sensitivity in the low-pressure regime (133.1 kPa^{-1}, <30 Pa), a short response time (50 ms), low hysteresis, and temperature stability (Fig. 4b–f). For a demonstration device of the pressure sensor arrays, we fabricated a pressure-sensor matrix of 64 pixels, each of which measured 36 mm^2, on a chessboard. The device could instantly detect the chess pieces' weight and location, showing potential utilization in the smart electronics field (Fig. 4g and h).

Despite the sensing performance of pressure sensors, stretchability and flexibility are vital for their practical applications, such as motion monitoring and dynamic pressure sensing.[73–76] In addition, wearable pressure sensors require excellent conformability and adhesion to a variety of surfaces.[77,78] CPHs of composite materials are a good candidate for excellent stretchability and flexibility.[56,79–81] By taking advantage of the high tunability of hydrogels, Wang *et al.* reported a ternary self-healing PAni composite as a combination of pressure sensors and strain sensors.[82] In the composite, phytic acid functions as a dopant to offer crosslinking points and increased electrical conductivity (0.12 S cm^{-1}) and strength. Polyacrylic acid is chosen as a soft and flexible counterpart to

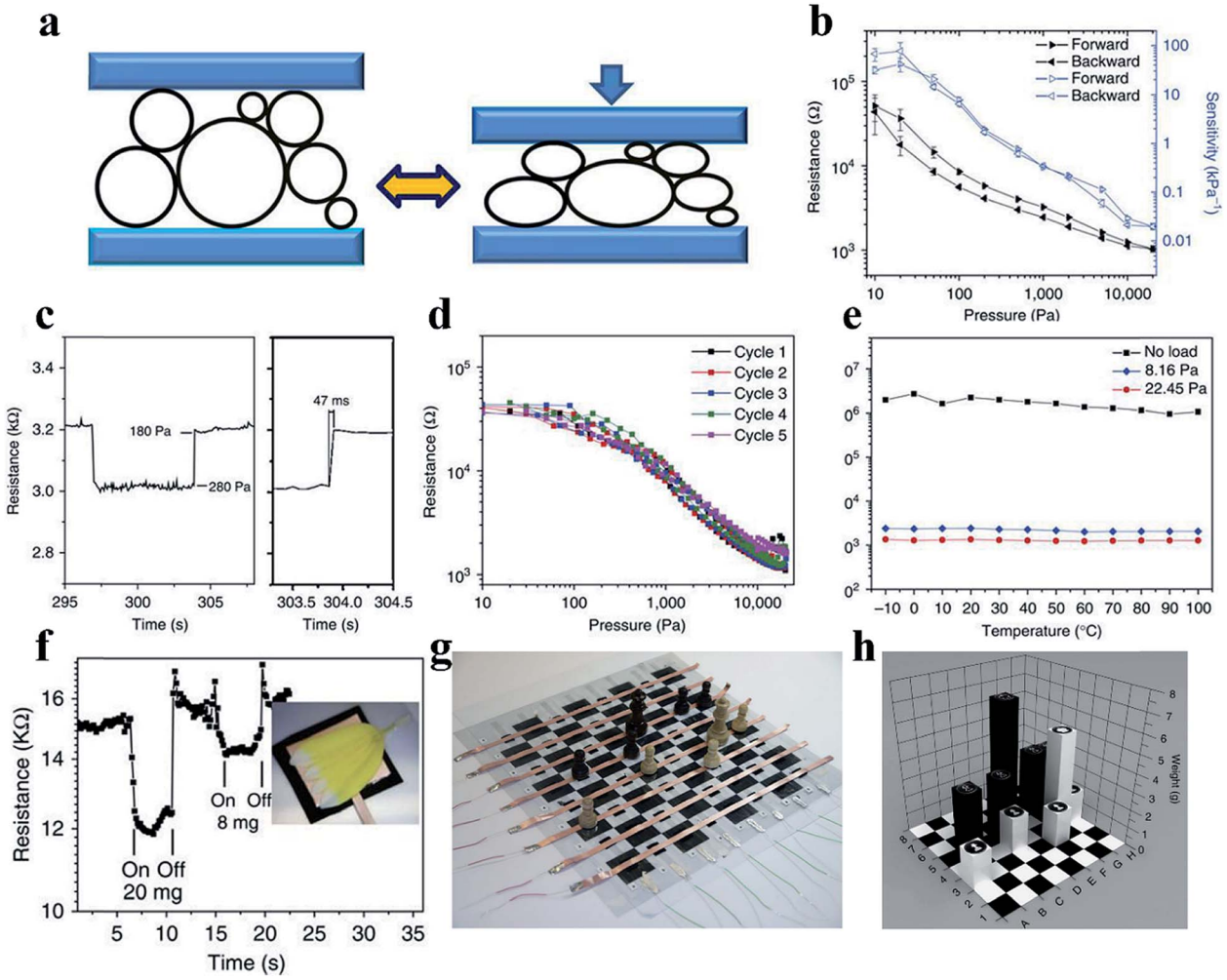

Fig. 4 Demonstration of a PPy-based pressure sensor. (a) The structural elasticity of the PPy hydrogel with hollow microstructures and the mechanism of the PPy-based pressure sensor. (b–e) show the resistance response and pressure sensitivity (b), response time (c), hysteresis (d) and temperature-dependent response (e) of the sensor. (f) The transient response of the micropatterned PPy to the application. (g and h) A prototype pressure sensor based on PPy situated on a chess board. Reprinted with permission from ref. 33 (copyright 2014 Macmillan Publishers Limited).

the rigid PAni chains, to improve the stretchability (460%). The introduction of polyacrylic acid could release the induced pressure by breaking weak hydrogen bonds instead of permanently damaging strong covalent bonds. The pressure sensor exhibited an ultrahigh sensitivity over a wide range (1.9 kPa^{-1}, >5 kPa) and is suitable for unprecedented dynamic and nonplanar pressure sensing. Notably, the composite is compatible with the solution-casting process for low-cost, large-scale fabrication. Furthermore, upon mechanical damage, self-healing capabilities allow the device to self-repair without external stimuli, which augments the device lifespan and reduces costs.[83]

3.2 Biosensor

Human body fluids are complex mixtures of a number of bioactive molecules, which are good indicators of some human diseases.[84–86] Engineering biosensors requires the capacity to transform chemical changes into electrical signals through a rational design that ensures remarkable sensitivity, high selectivity and biocompatibility.[87] Generally, most biosensors are based on enzymes, with which electrochemical signals can be detected through reactions with the target analytes.[88] Enzymatic biosensors demonstrate a high intrinsic selectivity and an excellent catalytic ability for different substances. The dopant-enabled nanostructured CPHs favor the immobilization of enzymes and the transfer of electrons, thus, enhancing the sensitivity of biosensors.[89] In addition, the excellent biocompatibility enables widespread applications of CPHs in the fields of biosensors, tissue engineering, and electronic skin.[90,91] The high water content and organic composition similar to those of the extracellular matrix endow CPHs with outstanding biocompatibility. Some natural molecules, such as phytic acid, are often utilized as a dopant and gelator, and the synthesized hydrogels show no obvious harm to living organisms/tissues in cytotoxicity testing.[92–94]

To date, CPHs have been an important component of sensor electrode platforms by means of the controlled spatial immobilization of enzymes. Biosensors featuring biocompatibility and sensitivity are desirable and can be expected from CPHs. For a successful example to realize these capabilities, we adopted a phytic-acid-doped PAni hydrogel modified with Pt nanoparticles (PtNPs) as an ultrasensitive glucose biosensor with a high sensitivity and rapid response time.[31] The PtNPs efficiently reduced the peroxide, the decomposition product from glucose oxidase, into analyzable water molecules (Fig. 5a).[95] Combining the conductivity, porosity, and biocompatibility of the PAni hydrogel with the catalytic properties of PtNPs, the biosensor exhibited an ultrahigh sensitivity of 96.1 $\mu A\ mM^{-1}\ cm^{-2}$. In the low glucose concentration range from 0.01 mM to 0.1 mM, the current output corresponded linearly with the glucose concentration change.

Multiple types of enzymes individually embedded into a hydrogel matrix can be used in an integrated sensor device to detect metabolites simultaneously. The addition of different enzymes to the PAni matrix allowed for the generation of signals in response to the concentration changes of a variety of analytes in the solution environment. Following a similar sensing mechanism, a multifunctional biosensor was then developed for detecting various human metabolites.[32] Enzymes were efficiently anchored to the PAni hydrogel in a high density by the carbonyl groups of glutaraldehyde (GA), which was used to crosslink enzymes and the hydrogel. Amperometric response results revealed that the PAni loaded with different enzymes could accurately and sensitively target specific metabolic molecules of uric acid, cholesterol and triglycerides with a fast response time of 3 s. Significantly, the PAni/enzyme composite possessed an ultrahigh sensitivity (322.8 $\mu A\ mM^{-1}\ cm^{-2}$) to uric acid from 0.07 mM to 1 mM with an outstanding linear relationship. Additionally, for two other molecules, the sensor also exhibited a linear relationship within a certain concentration range (0.3–9 mM for cholesterol and 0.2–5 mM for triglycerides); these ranges were broader than the normal ranges in human serum, promising a powerful biosensor platform for various biomedical applications.

The CPH itself and solution-based syntheses are compatible with inkjet and screen-printing techniques to offer facile micropatterning and scalability of production.[96] Printing techniques are favorable for low-cost, large-scale fabrication, which is more precise and material-saving without the need for additives. On the basis of the highly sensitive PAni/enzyme hybrid biosensor, we combined the advantages of the inkjet-printing technique with the selectivity of the PAni-based electrode and fabricated an all inkjet-printed, fast-processed integrated multiplex biosensor chip (5 min to fabricate 96 working electrodes) that could detect different analytes within a sensor chip.[6] The PAni hydrogel, PtNPs, and enzymes are printed onto a substrate through a drop-on-demand process (Fig. 5b). The sample drops on an inlet and flows along three channels with specific types of biosensors at the terminal, triggering highly sensitive responses to specific analytes. The biosensors detecting triglycerides, lactate, and glucose show sensitivities of 7.49, 3.94, and 5.03 $\mu A\ mM^{-1}\ cm^{-2}$, respectively (Fig. 5c). The prototype could not only distinguish distinct stimuli but also allow for repeating and reversible testing (Fig. 5d). These programmed fabrication properties of an inkjet printing system provide the possibility for chips with real-time testing and rapid processability, laying the foundation for building further-developed complex biomedical kits.

3.3 Gas sensor

Highly sensitive gas sensing is important for industrial hazardous gas monitoring, food status detection and healthcare monitoring. Traditional metal-oxide-based gas sensors have limitations such as a low sensitivity and high working temperature. Chemiresistive CPH-based gas sensors tend to favor high responses to gas molecules at room temperature. PAni or PAni-based composite materials are most widely utilized in sensitive ammonia gas sensors.[97–99] Exposure to ammonia gas leads to a dedoping process, where protons are removed from the PAni backbone, and the amount/mobility of charge carriers is decreased (Fig. 6b).[100] The porous nanostructures of CPHs enable the fast diffusion of gas molecules, and the high surface-

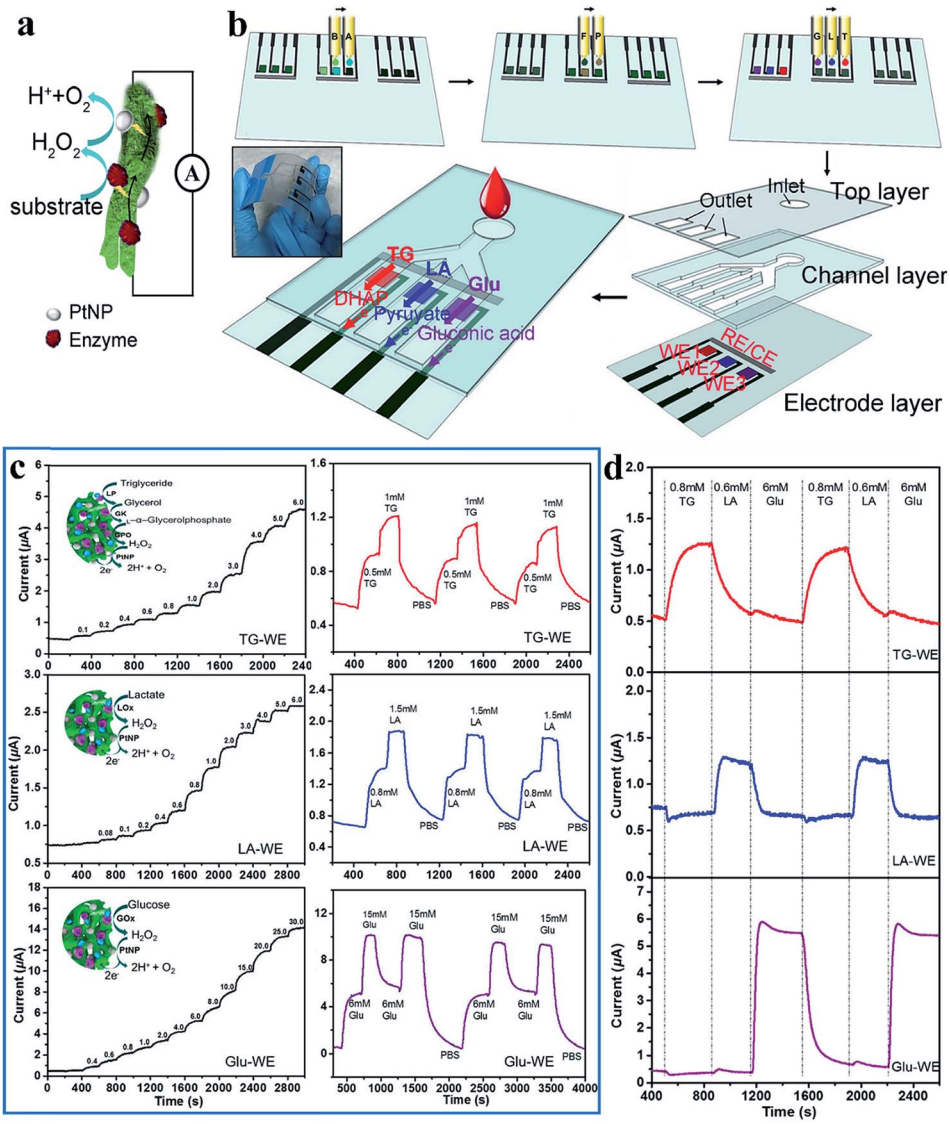

Fig. 5 Demonstration of the mechanism, fabrication and sensing performances of the inkjet-printed PAni-based biosensor. (a) Schematic illustration of the reaction mechanism of a PAni-based biosensor. (b) Schematic illustration of the fabrication of the inkjet-printed multiplexed PAni-based biosensor. Precursor solutions A and B; chloroplatinic acid (P) and formic acid (F) solutions; and enzyme solutions G (glucose oxidase solution), L (lactic oxidase solution), and T (mixed solution of lipase/glycerol kinase/L-α-glycerophosphate oxidase) are inkjet printed onto predefined areas of the working electrode. Three layers are then assembled to enable the multiplexed detection of metabolites. The inset shows a photo of the multiplexed sensors. (c) Instant response curves and repeatability of biosensors when detecting metabolite solutions of different concentrations. (d) The real-time signals collected from different electrodes when mixed metabolite solutions are pumped into the essay. Reprinted with permission from ref. 6 (copyright 2018 American Chemical Society).

to-volume ratio provides more sites for molecule adsorption and reaction. Therefore, nanostructured polymers show a substantially higher gas sensitivity than bulk materials, in which only the outermost surface can contact the gas.

Wang *et al.* reported a room-temperature ammonia gas sensor based on phytic-acid-doped PAni.[62] Pure PAni showed a resistive response of approximately 260% with a response time of 290 s. When incorporated with CeO_2 nanoparticles in a weight ratio to aniline of 4, the hybrid material exhibited a higher and faster response (a response of 6.5 and a response time 57.6 s). The improved sensing performances can be attributed to the p–n heterojunction within the core–shell structure. Notably, the sensor showed outstanding long-term stability with sensing capabilities maintained after 30 cycles in 15 d, which is due to the doping and crosslinking effects on the polymer chains.

We recently reported the device design of a highly sensitive PAni-based amine gas sensor for wireless food spoilage detection by smartphones.[7] We adopted iron(III) *p*-toluene sulfonate hexahydrate as the dopant; the iron(III) ion acts as the initiator of polymerization, resulting in a nanostructured PAni with an initially higher conductivity (Fig. 6a). Since the ammonia and biogenic amines released from food result in a dedoping process, the PAni experienced a resistive increase with

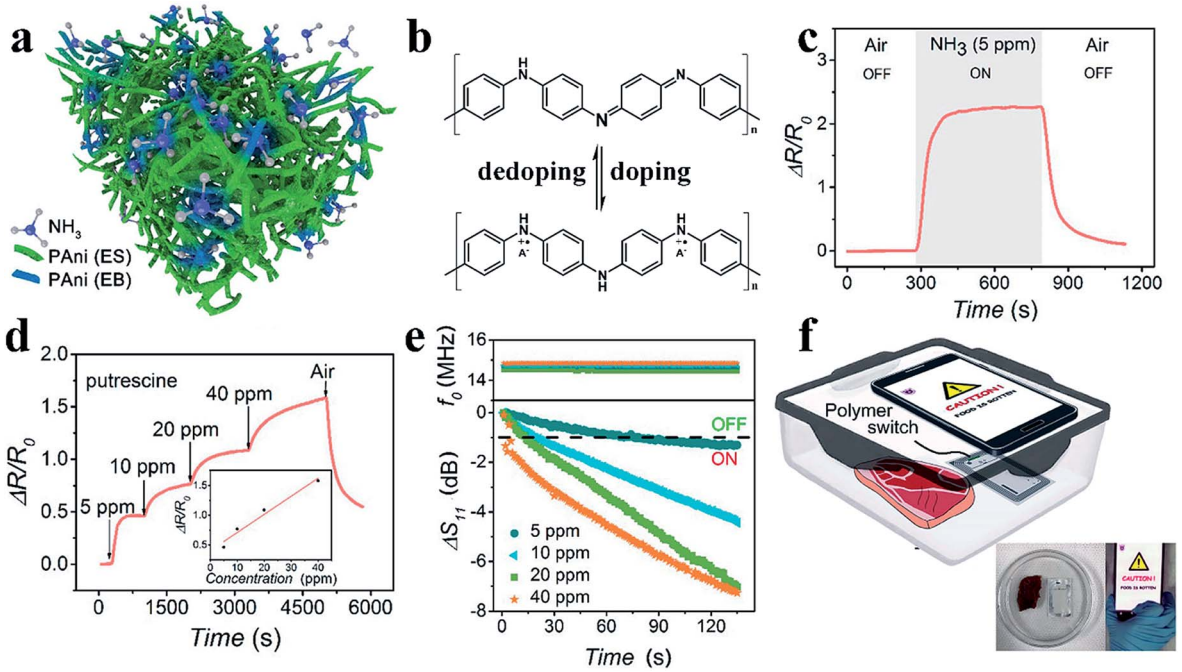

Fig. 6 Demonstration of the PAni-based amine gas sensor. (a) A schematic illustration of the general sensing mechanism of the PTS-doped PAni-based gas sensor. (b) The reversible doping/dedoping process of PAni results in the conversion between conductors and insulators. (c and d) The resistance responses of PAni to ammonia and putrescine. (e) The real-time responses to different concentrations of ammonia of the PAni-modified NFC tag in terms of the reflection coefficient and resonant frequency. (f) The application of modified NFC tags to detect meat spoilage with a smartphone. Reprinted with permission from ref. 7 (copyright 2018 American Chemical Society).

a sensitivity of $\Delta R/R_0$ = 225% toward 5 ppm ammonia and unprecedented sensitivities of 46% and 17% toward 5 ppm putrescine and cadaverine, respectively. Excellent reversibility and selectivity were also obtained (Fig. 6c and d). With high resistive responses, the PAni-based gas sensor can be incorporated with near field communication (NFC) technology to realize intelligent, convenient sensing assisted by mobile phones.[101,102] The PAni hydrogel readily forms micropatterns on NFC tags *via* an inkjet printing process. When PAni, with a low resistance, is printed onto the circuit, less signal resonates, and the tag is unreadable because of the mismatch in the impedance of the NFC tag and that of the reader (Fig. 6e). In the presence of amine gas, the high resistive response of PAni rematches the impedances and switches on the NFC tag, sending an alarm back to the mobile phone (Fig. 6f). The sensitive switchability of the PAni-based sensor suggests great potential for use in the field of intelligent wireless detection and sensing.

Fig. 7 Outlook of the future development and investigation of CPH-based sensor technology. Future development of CPH-based sensor technology lies in the improvement of sensing functions (improving sensing abilities and achieving multifunctional sensing systems as well as other novel functions) and broadening of the application form in daily lives (developing wearable devices and realizing self-powered/wireless sensors).

4. Conclusions

In conclusion, the CPH stands out as a promising platform for various sensor technologies benefiting from the unique combination of the intrinsic merits of hydrogels and organic conductors. The nature of the hydrogel structure such as hydrophilicity, porosity, and biocompatibility serve as a solid framework for multi-component systems, which further increase the diversity of properties and functions of the CPH platform. On the basis of CPH's highly tunable 3D network, introducing dopants is an effective method that greatly enhances the CPH's interchain electron/ion conductivity benefiting from the ordering of the polymer chains and the conductive dopant molecules, as well as increases the mechanical strength and stabilizes the hydrogel matrix. In

addition, dopants bring along a novel sensing mechanism, for example, the doping/dedoping mechanism, where hydrogels directly react with target objects by utilizing the conductivity tuning principles, providing an avenue to sensing.

Key challenges to practical applications still reside in the requirement of a high sensitivity over a broad range and a multiple sensing ability (Fig. 7). In this sense, CPHs may be further tuned toward an efficient system with a better sensing performance by rational compositional design at the molecular level. Hydrogel network engineering such as investigating effective moieties and dopants, modification strategies, and a better understanding of the sensing mechanism are to be developed in order to provide opportunities for more innovations in multimodal CPH-based sensors. CPHs can be easily micropatterned for integrated devices (*e.g.*, microneedles and transdermal sensors), demonstrating great potential for use in multifunctional platforms not limited to sensing. Tuning and improving hydrogel mechanics remain another challenge. Mechanical properties are not only critical in force/strain sensors but also play a key role in extending all types of sensors to wearable devices. Moreover, CPH-based sensors with other unique capabilities such as self-healing, self-powering, biodegradability, and wireless transmission are expected to further expand the material's applications.[103,104] Future advances in sensing performance (*e.g.*, sensitivity, selectivity, and stability) and system integration, combined with technology support by chemistry and materials engineering, are envisioned for accurate, real-time and consistent monitoring in healthcare applications.

Conflicts of interest

There are no conflicts to declare.

Acknowledgements

G. Y. acknowledges the financial support from the Welch Foundation award F-1861, Alfred P. Sloan Research Fellowship, and Camille Dreyfus Teacher-Scholar Award. L. P. acknowledges the financial support of the National Natural Science Foundation of China under Grants 61825403 and 61674078, the National Key Research and Development program of China under Grant 2017YFA0206302, and the PAPD program.

References

1 H. Yuk, B. Lu and X. Zhao, *Chem. Soc. Rev.*, 2019, **48**, 1642–1667.
2 Y. Shi and G. Yu, *Chem. Mater.*, 2016, **28**, 2466–2477.
3 S. Lin, H. Yuk, T. Zhang, G. A. Parada, H. Koo, C. Yu and X. Zhao, *Adv. Mater.*, 2016, **28**, 4497–4505.
4 F. Zhao, Y. Shi, L. Pan and G. Yu, *Acc. Chem. Res.*, 2017, **50**, 1734–1743.
5 Y. Shi, L. Peng and G. Yu, *Nanoscale*, 2015, **7**, 12796–12806.
6 L. Li, L. Pan, Z. Ma, K. Yan, W. Cheng, Y. Shi and G. Yu, *Nano Lett.*, 2018, **18**, 3322–3327.
7 Z. Ma, P. Chen, W. Cheng, K. Yan, L. Pan, Y. Shi and G. Yu, *Nano Lett.*, 2018, **18**, 4570–4575.
8 Y. Shi, L. Peng, Y. Ding, Y. Zhao and G. Yu, *Chem. Soc. Rev.*, 2015, **44**, 6684–6696.
9 L. Lai, Y. Zhao, S. Ying, L. Li, Z. Ma and L. Pan, *RSC Adv.*, 2018, **8**, 18714–18722.
10 P. Li, Z. Jin, L. Peng, F. Zhao, D. Xiao, Y. Jin and G. Yu, *Adv. Mater.*, 2018, **30**, 1800124.
11 C. Yu, C. Wang, X. Liu, X. Jia, S. Naficy, K. Shu, M. Forsyth and G. G. Wallace, *Adv. Mater.*, 2016, **28**, 9349–9355.
12 F. Zhao, X. Zhou, Y. Shi, X. Qian, M. Alexander, X. Zhao, S. Mendez, R. Yang, L. Qu and G. Yu, *Nat. Nanotechnol.*, 2018, **13**, 489.
13 X. Zhou, F. Zhao, Y. Guo, Y. Zhang and G. Yu, *Energy Environ. Sci.*, 2018, **11**, 1985–1992.
14 Y. Shi, C. Ma, Y. Du and G. Yu, *J. Mater. Chem. B*, 2017, **5**, 3541–3549.
15 C. Ma, Y. Shi, D. A. Pena, L. Peng and G. Yu, *Angew. Chem., Int. Ed.*, 2015, **54**, 7376–7380.
16 X. Yi, J. Dai, Y. Han, M. Xu, X. Zhang, S. Zhen, Z. Zhao, X. Lou and F. Xia, *Commun. Biol.*, 2018, **1**, 202.
17 Y. Wang, Y. Shi, L. Pan, M. Yang, L. Peng, S. Zong, Y. Shi and G. Yu, *Nano Lett.*, 2014, **14**, 4803–4809.
18 X. Yao, L. Chen, J. Ju, C. Li, Y. Tian, L. Jiang and M. Liu, *Adv. Mater.*, 2016, **28**, 7383–7389.
19 Y. Zhao, B. Liu, L. Pan and G. Yu, *Energy Environ. Sci.*, 2013, **6**, 2856–2870.
20 H. R. Culver, J. R. Clegg and N. A. Peppas, *Acc. Chem. Res.*, 2017, **50**, 170–178.
21 N. Annabi, A. Tamayol, J. A. Uquillas, M. Akbari, L. E. Bertassoni, C. Cha, G. Camci-Unal, M. R. Dokmeci, N. A. Peppas and A. Khademhosseini, *Adv. Mater.*, 2014, **26**, 85–124.
22 Y. Shi, J. Zhang, L. Pan, Y. Shi and G. Yu, *Nano Today*, 2016, **11**, 738–762.
23 K. Zhou, Y. He, Q. Xu, Q. Zhang, A. Zhou, Z. Lu, L.-K. Yang, Y. Jiang, D. Ge, X. Y. Liu and H. Bai, *ACS Nano*, 2018, **12**, 5888–5894.
24 A. J. Heeger, *J. Phys. Chem. B*, 2001, **105**, 8475–8491.
25 A. G. MacDiarmid, *Angew. Chem., Int. Ed.*, 2001, **40**, 2581–2590.
26 M. Canales, J. Torras, G. Fabregat, A. Meneguzzi and C. Alemán, *J. Phys. Chem. B*, 2014, **118**, 11552–11562.
27 J. L. Bredas and G. B. Street, *Acc. Chem. Res.*, 1985, **18**, 309–315.
28 M. Nowak, S. D. D. V. Rughooputh, S. Hotta and A. J. Heeger, *Macromolecules*, 1987, **20**, 965–968.
29 Y. Cao, P. Smith and A. J. Heeger, *Synth. Met.*, 1993, **57**, 3514–3519.
30 Y. Wang, Y. Shi, L. Pan, Y. Ding, Y. Zhao, Y. Li, Y. Shi and G. Yu, *Nano Lett.*, 2015, **15**, 7736–7741.
31 D. Zhai, B. Liu, Y. Shi, L. Pan, Y. Wang, W. Li, R. Zhang and G. Yu, *ACS Nano*, 2013, **7**, 3540–3546.
32 L. Li, Y. Wang, L. Pan, Y. Shi, W. Cheng, Y. Shi and G. Yu, *Nano Lett.*, 2015, **15**, 1146–1151.
33 L. Pan, A. Chortos, G. Yu, Y. Wang, S. Isaacson, R. Allen, Y. Shi, R. Dauskardt and Z. Bao, *Nat. Commun.*, 2014, **5**, 3002.

34 L. Li, Y. Shi, L. Pan, Y. Shi and G. Yu, *J. Mater. Chem. B*, 2015, **3**, 2920–2930.
35 P. Fattahi, G. Yang, G. Kim and M. R. Abidian, *Adv. Mater.*, 2014, **26**, 1846–1885.
36 L. Pan, L. Pu, Y. Shi, S. Song, Z. Xu, R. Zhang and Y. Zheng, *Adv. Mater.*, 2007, **19**, 461–464.
37 L. Pan, H. Qiu, C. Dou, Y. Li, L. Pu, J. Xu and Y. Shi, *Int. J. Mol. Sci.*, 2010, **11**, 2636–2657.
38 F. Zhao, J. Bae, X. Zhou, Y. Guo and G. Yu, *Adv. Mater.*, 2018, **30**, 1801796.
39 K. P. R. Nilsson, J. Rydberg, L. Baltzer and O. Inganäs, *Proc. Natl. Acad. Sci. U. S. A.*, 2004, **101**, 11197–11202.
40 S. Ghosh, J. Rasmusson and O. Inganäs, *Adv. Mater.*, 1998, **10**, 1097–1099.
41 T. Dai, X. Jiang, S. Hua, X. Wang and Y. Lu, *Chem. Commun.*, 2008, 4279–4281.
42 J. Huang and R. B. Kaner, *J. Am. Chem. Soc.*, 2004, **126**, 851–855.
43 J. Huang and M. Wan, *J. Polym. Sci., Part A: Polym. Chem.*, 1999, **37**, 1277–1284.
44 L. Pan, G. Yu, D. Zhai, H. R. Lee, W. Zhao, N. Liu, H. Wang, B. C.-K. Tee, Y. Shi, Y. Cui and Z. Bao, *Proc. Natl. Acad. Sci. U. S. A.*, 2012, **109**, 9287–9292.
45 J. Zhang, Y. Shi, Y. Ding, L. Peng, W. Zhang and G. Yu, *Adv. Energy Mater.*, 2017, **7**, 1602876.
46 J. Bae, Y. Li, J. Zhang, X. Zhou, F. Zhao, Y. Shi, J. B. Goodenough and G. Yu, *Angew. Chem., Int. Ed.*, 2018, **57**, 2096–2100.
47 J. Bae, Y. Li, F. Zhao, X. Zhou, Y. Ding and G. Yu, *Energy Storage Materials*, 2018, **15**, 46–52.
48 J. Huang, S. Virji, B. H. Weiller and R. B. Kaner, *J. Am. Chem. Soc.*, 2003, **125**, 314–315.
49 Y. Lu, Q. Zheng, J. Wu and Y. Yu, *Electrochim. Acta*, 2018, **265**, 594–600.
50 Y. Shi, X. Zhou, J. Zhang, A. M. Bruck, A. C. Bond, A. C. Marschilok, K. J. Takeuchi, E. S. Takeuchi and G. Yu, *Nano Lett.*, 2017, **17**, 1906–1914.
51 L. Nyholm, G. Nyström, A. Mihranyan and M. Strømme, *Adv. Mater.*, 2011, **23**, 3751–3769.
52 Y. Shi, L. Pan, B. Liu, Y. Wang, Y. Cui, Z. Bao and G. Yu, *J. Mater. Chem. A*, 2014, **2**, 6086–6091.
53 Y. Lu, W. He, T. Cao, H. Guo, Y. Zhang, Q. Li, Z. Shao, Y. Cui and X. Zhang, *Sci. Rep.*, 2014, **4**, 5792.
54 Y. An, K. Iwashita and H. Okuzaki, *Multifunct. Mater.*, 2018, **2**, 014001.
55 T. Long, Y. Li, X. Fang and J. Sun, *Adv. Funct. Mater.*, 2018, **28**, 1804416.
56 J. Duan, X. Liang, J. Guo, K. Zhu and L. Zhang, *Adv. Mater.*, 2016, **28**, 8037–8044.
57 H. Shi, Z. Fang, X. Zhang, F. Li, Y. Tang, Y. Zhou, P. Wu and G. Yu, *Nano Lett.*, 2018, **18**, 3193–3198.
58 Z. Wang, H. Zhou, J. Lai, B. Yan, H. Liu, X. Jin, A. Ma, G. Zhang, W. Zhao and W. Chen, *J. Mater. Chem. C*, 2018, **6**, 9200–9207.
59 Z. Chen, J. W. F. To, C. Wang, Z. Lu, N. Liu, A. Chortos, L. Pan, F. Wei, Y. Cui and Z. Bao, *Adv. Energy Mater.*, 2014, **4**, 1400207.
60 R. Zhang, L. Wang, Z. Shen, M. Li, X. Guo and Y. Yao, *Macromol. Rapid Commun.*, 2017, **38**, 1700455.
61 B. Liu, P. Soares, C. Checkles, Y. Zhao and G. Yu, *Nano Lett.*, 2013, **13**, 3414–3419.
62 L. Wang, H. Huang, S. Xiao, D. Cai, Y. Liu, B. Liu, D. Wang, C. Wang, H. Li, Y. Wang, Q. Li and T. Wang, *ACS Appl. Mater. Interfaces*, 2014, **6**, 14131–14140.
63 Y. Shi, J. Zhang, A. M. Bruck, Y. Zhang, J. Li, E. A. Stach, K. J. Takeuchi, A. C. Marschilok, E. S. Takeuchi and G. Yu, *Adv. Mater.*, 2017, **29**, 1603922.
64 Y. Zhao, L. Cao, L. Li, W. Cheng, L. Xu, X. Ping, L. Pan and Y. Shi, *Sensors*, 2016, **16**, 1787.
65 M. L. Hammock, A. Chortos, B. C.-K. Tee, J. B.-H. Tok and Z. Bao, *Adv. Mater.*, 2013, **25**, 5997–6038.
66 J.-Y. Sun, C. Keplinger, G. M. Whitesides and Z. Suo, *Adv. Mater.*, 2014, **26**, 7608–7614.
67 A. Chortos, J. Liu and Z. Bao, *Nat. Mater.*, 2016, **15**, 937–950.
68 W. Cheng, L. Yu, D. Kong, Z. Yu, H. Wang, Z. Ma, Y. Wang, J. Wang, L. Pan and Y. Shi, *IEEE Electron Device Lett.*, 2018, **39**, 1069–1072.
69 W. Cheng, J. Wang, Z. Ma, K. Yan, Y. Wang, H. Wang, S. Li, Y. Li, L. Pan and Y. Shi, *IEEE Electron Device Lett.*, 2018, **39**, 288–291.
70 Z. Ma, S. Li, H. Wang, W. Cheng, Y. Li, L. Pan and Y. Shi, *J. Mater. Chem. B*, 2019, **7**, 173–197.
71 Z. Wang, J. Chen, L. Wang, G. Gao, Y. Zhou, R. Wang, T. Xu, J. Yin and J. Fu, *J. Mater. Chem. B*, 2019, **7**, 24–29.
72 S. Jung, J. H. Kim, J. Kim, S. Choi, J. Lee, I. Park, T. Hyeon and D.-H. Kim, *Adv. Mater.*, 2014, **26**, 4825–4830.
73 Q. Rong, W. Lei and M. Liu, *Chem.–Eur. J.*, 2018, **24**, 16930–16943.
74 Z. Wang, J. Chen, Y. Cong, H. Zhang, T. Xu, L. Nie and J. Fu, *Chem. Mater.*, 2018, **30**, 8062–8069.
75 A. Frutiger, J. T. Muth, D. M. Vogt, Y. Mengüç, A. Campo, A. D. Valentine, C. J. Walsh and J. A. Lewis, *Adv. Mater.*, 2015, **27**, 2440–2446.
76 M. S. Sarwar, Y. Dobashi, C. Preston, J. K. M. Wyss, S. Mirabbasi and J. D. W. Madden, *Sci. Adv.*, 2017, **3**, e1602200.
77 Y.-Z. Zhang, K. H. Lee, D. H. Anjum, R. Sougrat, Q. Jiang, H. Kim and H. N. Alshareef, *Sci. Adv.*, 2018, **4**, eaat0098.
78 Z. Lei and P. Wu, *Nat. Commun.*, 2018, **9**, 1134.
79 G. Ge, Y. Zhang, J. Shao, W. Wang, W. Si, W. Huang and X. Dong, *Adv. Funct. Mater.*, 2018, **28**, 1802576.
80 S. Xia, S. Song and G. Gao, *Chem. Eng. J.*, 2018, **354**, 817–824.
81 Y. Si, L. Wang, X. Wang, N. Tang, J. Yu and B. Ding, *Adv. Mater.*, 2017, **29**, 1700339.
82 T. Wang, Y. Zhang, Q. Liu, W. Cheng, X. Wang, L. Pan, B. Xu and H. Xu, *Adv. Funct. Mater.*, 2017, **28**, 1705551.
83 Y. Shi, M. Wang, C. Ma, Y. Wang, X. Li and G. Yu, *Nano Lett.*, 2015, **15**, 6276–6281.
84 M. Bariya, H. Y. Y. Nyein and A. Javey, *Nat. Electron.*, 2018, **1**, 160–171.
85 Y. Yang and W. Gao, *Chem. Soc. Rev.*, 2019, **48**, 1465–1491.

86 Y. J. Heo, H. Shibata, T. Okitsu, T. Kawanishi and S. Takeuchi, *Proc. Natl. Acad. Sci. U. S. A.*, 2011, **108**, 13399–13403.
87 A. Yang, Y. Li, C. Yang, Y. Fu, N. Wang, L. Li and F. Yan, *Adv. Mater.*, 2018, **30**, 1800051.
88 A.-M. Pappa, O. Parlak, G. Scheiblin, P. Mailley, A. Salleo and R. M. Owens, *Trends Biotechnol.*, 2018, **36**, 45–59.
89 M. Wang, M. Cui, W. Liu and X. Liu, *J. Electroanal. Chem.*, 2019, **832**, 174–181.
90 T. Nezakati, A. Seifalian, A. Tan and A. M. Seifalian, *Chem. Rev.*, 2018, **118**, 6766–6843.
91 B. Guo and P. X. Ma, *Biomacromolecules*, 2018, **19**, 1764–1782.
92 K.-H. Sun, Z. Liu, C. Liu, T. Yu, T. Shang, C. Huang, M. Zhou, C. Liu, F. Ran, Y. Li, Y. Shi and L. Pan, *Sci. Rep.*, 2016, **6**, 23931.
93 L. E. Strong, S. N. Dahotre and J. L. West, *J. Controlled Release*, 2014, **178**, 63–68.
94 G. Guo, Y. Chen, X. Liu, D. Yu Zhu, B. Zhang, N. Lin and L. Gao, *J. Mater. Chem. B*, 2018, **6**, 8043–8054.
95 Y. Chen, L. Li, L. Zhang and J. Han, *Colloid Polym. Sci.*, 2018, **296**, 567–574.
96 F. Zhu, J. Lin, Z. L. Wu, S. Qu, J. Yin, J. Qian and Q. Zheng, *ACS Appl. Mater. Interfaces*, 2018, **10**, 13685–13692.
97 M. Eising, C. E. Cava, R. V. Salvatierra, A. J. G. Zarbin and L. S. Roman, *Sens. Actuators, B*, 2017, **245**, 25–33.
98 D. K. Bandgar, S. T. Navale, S. R. Nalage, R. S. Mane, F. J. Stadler, D. K. Aswal, S. K. Gupta and V. B. Patil, *J. Mater. Chem. C*, 2015, **3**, 9461–9468.
99 S. Bai, C. Sun, P. Wan, C. Wang, R. Luo, Y. Li, J. Liu and X. Sun, *Small*, 2015, **11**, 306–310.
100 N. R. Tanguy, M. Thompson and N. Yan, *Sens. Actuators, B*, 2018, **257**, 1044–1064.
101 R. Zhu, M. Azzarelli Joseph and M. Swager Timothy, *Angew. Chem., Int. Ed.*, 2016, **55**, 9662–9666.
102 L. Zhang, B. Gupta, B. Goudeau, N. Mano and A. Kuhn, *J. Am. Chem. Soc.*, 2018, **140**, 15501–15506.
103 Z. Deng, Y. Guo, X. Zhao, P. X. Ma and B. Guo, *Chem. Mater.*, 2018, **30**, 1729–1742.
104 W. Xu, L.-B. Huang, M.-C. Wong, L. Chen, G. Bai and J. Hao, *Adv. Energy Mater.*, 2017, **7**, 1601529.